Available online at www.sciencedirect.com
SCIENCE DIRECT®
Chemical Physics Letters 404 (2005) 30–34
CHEMICAL PHYSICS LETTERS
www.elsevier.com/locate/cplett

Synthesis and optoelectronic properties of arrayed p-type ZnO nanorods grown on ZnO film/Si wafer in aqueous solutions

Chin-Ching Lin, Hung-Pei Chen, San-Yuan Chen *

Department of Materials Science and Engineering, National Chiao Tung University, 1001 Ta-hsueh Road, Hsinchu 300, Taiwan, Republic of China

Received 20 September 2004; in final form 10 January 2005

Abstract

Highly arrayed nitrogen-doped ZnO nanorods were fabricated on Si buffered with ZnO film by combining wet-chemical process with post-treated by NH_3 plasma. The X-ray photoelectron spectroscopy measurement demonstrates that the nitrogen-doped ZnO nanorods have been formed due to nitrogen diffusion through surface adsorption or defect routes. The photoluminescence spectra indicate that a strong UV emission peak around 3.31 eV with negligible deep level emission can be obtained for the nitrogen-doped ZnO nanorods compared to that of the untreated sample. The I–V measurements indicate that the p-type ZnO nanorods with a smaller threshold voltage of 1.5 V can be obtained.

1. Introduction

One-dimensional (1D) semiconductor nanostructures have been extensively studies for their potential applications in manufacturing electronic and optoelectronic devices [1–3]. Zinc oxide is an important electronic and photonic material because of its wide direct band gap of 3.37 eV and a relatively large exciton binding energy of 60 meV. ZnO nanowires are expected to further lower the lasing threshold because of quantum effects that result in the enhancement of density of states near the band edges and radiative recombination due to carrier confinement [4]. Recently, a variety of methods have been employed, including radio frequency sputtering, metal-organic chemical vapor deposition (MOCVD), and catalyst-assisted vapor phase transport techniques, to fabricate highly oriented ZnO nanowires (or nanorods) on various substrates [5,6]. However, those are expensive and energy-consuming processes since they are operated under extreme conditions.

On the other hand, wet-chemical approaches have been widely used for the fabrication of large oriented arrays of ZnO nanorods on polycrystalline (or single-crystalline) substrates because the preparation of ZnO via solution chemical routes provides a promising option for large-scale production [7,8]. However, it was noted that without suitable treatment on the substrates, highly oriented ZnO nanorods has been rarely grown on a Si wafer from aqueous solutions.

Although ZnO was reported to be the most potential material to realize the next generation in UV semiconductor laser, most of the ZnO crystal is an n-type because it contains significant concentrations of shallow donors and native defects (Zn interstitials, O vacancies). Therefore, it is necessary to grow high-quality p-type ZnO. However, unfortunately, most 1D nanomaterials (nanowires or nanorods) have been paraded as 'perfect-like' or 'defects-free' nanocrystals so that there are rarely efficient methods to fabricate p-type ZnO nanoscale nanostructures via doping the grown ZnO nanorods because no suitable diffusion paths can provide for the doping or incorporation of impurities into ZnO nanorods except for in situ growth of doped-ZnO via VLS process [9,10].

* Corresponding author. Fax: +886 3 5725490.
E-mail address: sychen@cc.nctu.edu.tw (S.-Y. Chen).

0009-2614/$ - see front matter © 2005 Elsevier B.V. All rights reserved.
doi:10.1016/j.cplett.2005.01.047

Therefore, in this work, a simple process by combining the aqueous solution process with NH_3 plasma treatment was proposed to develop well-aligned p-type ZnO nanorods on a Si substrate buffered with ZnO film. To our best knowledge, it is for the first time to report the doping of nitrogen into ZnO nanorods and demonstrate that the nitrogen-doped ZnO nanorods exhibit p-type characteristics.

2. Experiments

Following the procedure proposed by Vayssieres [7], stock solutions from equimolecular aqueous solution of zinc nitrate hexahydrate ($Zn(NO_3)_2 \cdot 6H_2O$) and hexamethylenetetramine ($C_6H_{12}N_4$, HMT) were prepared for the growth of ZnO nanorods on p-type Si (1 0 0) substrates buffered with sputtered ZnO film (ZnO_f/Si). The n-ZnO films exhibited an n-type carrier concentration of 3×10^{17} cm^{-3} and mobility of 36 cm^2 V^{-1} s^{-1}. Subsequently, the ZnO-coated Si substrates were placed in the glass bottles filled with 0.01 M aqueous solution at 75 °C for 10 h. After grown, the ZnO nanorods were exposed to NH_3 plasma for 30, 60, 90, 180, and 900 s. For the plasma treatment, the substrate temperature, total gas pressure and RF power were maintained at 300 °C, 300 mTorr and 250 W, respectively. Ohmic contacts were fabricated simply by sputtering indium (In) and aurum (Au)/indium metal on n-ZnO films and p-ZnO nanorods. The contact electrodes have the area of 1×10^{-4} cm^2 and the average nanorod density was estimated to be about 10^9 cm^{-2}. After metallization of n-ZnO films, the gaps between the nanorods were filled with polystyrene (PS) beads (diameter ~50 nm). Contact metal was sputtered on the tip of ZnO nanorods through a shadow mask, resulting in a continuous conductivity layer on the PS beads and the tip of nanorods. Next, the PS beads can be removed by immersing the sample in toluene. Finally, good ohmic contacts on both n-ZnO films and p-type ZnO nanorods were made by rapidly thermal annealing at 350 °C for 20 min in nitrogen atmosphere.

The morphology and microstructures of the ZnO nanorods were examined by field-emission scanning electron microscopy (FE-SEM) using JAM-6500F and transmission electron microscope (TEM) with Philips TECNAI 20. Photoluminescence of the ZnO nanorods were performed by the excitation from 325 nm He–Cd laser at room temperature. The chemical compositions and relative intensity ratio of internal N (N_i) to surface N (N_f) on various etching time were examined by X-ray photoelectron spectroscopy (XPS). I–V characteristics curve of the samples was measured by applying DC voltage to the device using a HP-4156 and each datum was averaged by measuring 10 times.

3. Results and discussion

The ZnO nanorods present single crystalline structure and a well-defined hexagonal plane with a homogeneous diameter of approximately 60–70 nm. The cross-sectional scanning electron microcopy (SEM) image in Fig. 1a shows that the highly oriented ZnO nanorods with a uniform length of 500–520 nm are perpendicularly grown to the substrate. In addition, it was found that by controlling the experimental conditions, highly arrayed ZnO nanorods or nanowires with different aspect ratios can be grown from the chemical aqueous solution [11]. A close observation on the microstructure of the ZnO nanorods, as shown in Fig. 1b, reveals that the surface morphology of ZnO nanorods shows a waved shape structure with 0.5–1 nm roughnesses. In addition, some stacking faults are also observed (marked with arrows). However, these small surface roughness and stacking faults seem not to affect the crystal quality of ZnO nanorods because the selected-area electron diffraction pattern in the inset of Fig. 1b reveals that the ZnO nanorods still exhibit a single crystalline structure. Fig. 1b clearly describes the perpendicular directional growth of the ZnO nanorods where the

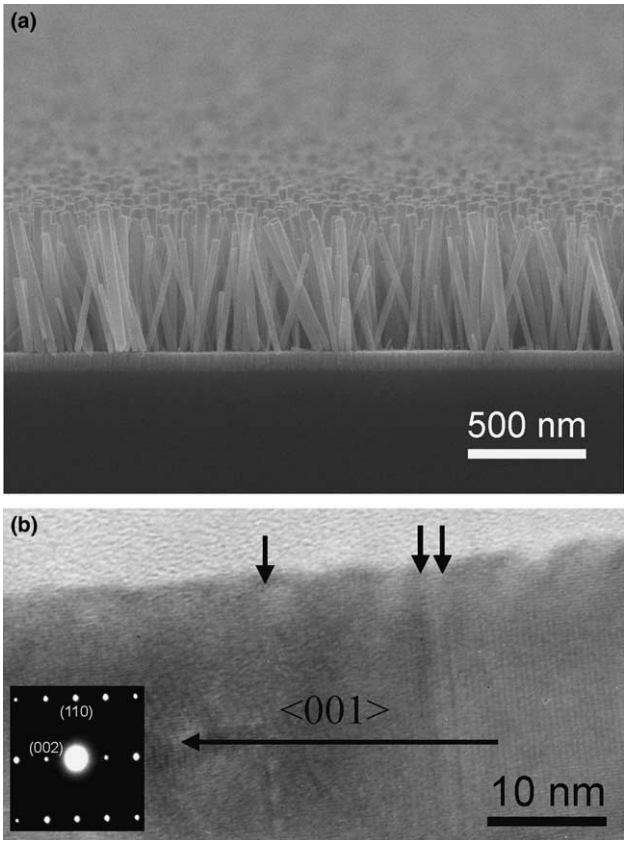

Fig. 1. Cross-sectional scanning electron microcopy (SEM) micrograph of (a) ZnO nanorods/ZnO film/Si, (b) surface microstructure and stacking faults (marked with arrows) of ZnO nanorods. The inset image of (b) displays SAED pattern.

singular fringes spacing is about 0.51 nm, which is nearly consistent with the *c*-axis parameter in hexagonal ZnO structure ($c = 0.521$ nm in ZnO wurtzite structure), indicating that $\langle 0\,0\,1\rangle$ is the preferred growth direction for the ZnO nanorods, in consistence with XRD patterns that shows a single strong ZnO (0 0 2) peak at $2\theta = 34.4°$ (not shown here).

Fig. 2a illustrates the photoluminescence (PL) property of ZnO nanorods at room temperature. The PL spectrum of non-plasma ZnO nanorods presents a weak ultraviolet (UV) emission peak at 3.28 eV and a relatively strong deep-level emission peak at 2.10 eV. The UV emission peak of ZnO is generally attributed to an exciton-related activity [12], and the deep level emission may be due to the transitions of native defects such as oxygen vacancies and zinc interstitials. In addition, the imperfect boundaries in ZnO nanorods would cause the unstable surface status to trap impurities and further damage the optical property, especially for the nanoscale ZnO nanorods. In contrast, it was found that the peak intensity of the UV emission increases with the plasma duration up to 90 s but the deep level emission in all plasma-treated samples tends to disappear, indicating that the native defects or impurities, contributing to visible transition, can be much reduced by NH_3 plasma treatment. As shown in Fig. 2b, a maximum relative PL ratio (peak intensity of ultraviolet emission (I_{UV}) to that of deep level emission (I_{DLE})) shows up around 90–120 s, implying that the plasma-treated ZnO nanorods exhibit much better PL properties than that of non-plasma sample. The improvement in the optical properties of ZnO nanorods with the plasma treatment may be attributed to the reduction of the defect concentration due to the occupation of N ions on the defect sites, i.e., oxygen vacancies, which will be further elucidated later. However, a further increase in plasma duration such as 180 s would result in the decrease in the relative PL ratio that is probably related to the plasma etching as revealed by the SEM image in Fig. 2c where the ZnO nanorods were deteriorated that is in contrast to the ZnO nanorods with the plasma-treated duration less than 90 s, well-aligned ZnO nanorods with well-defined hexagonal plane remains unchanged with an average length of 500 nm, similar to that without NH_3 plasma treatment.

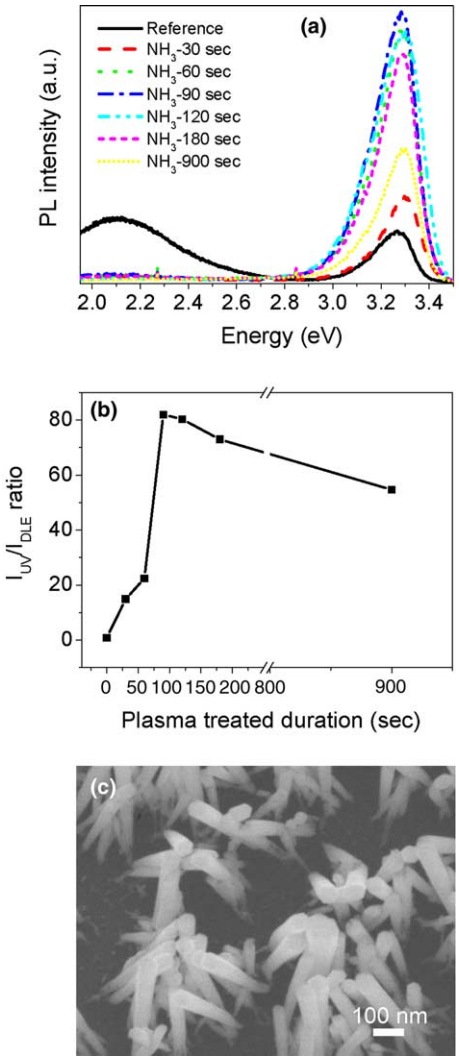

Fig. 2. (a) Room-temperature PL spectra and (b) PL ratio of I_{UV}/I_{DEL} for ZnO nanorods with and without NH_3 plasma treatment. (c) The FESEM surface morphology of ZnO nanorods with NH_3 plasma treatment of $t = 180$ s.

Fig. 3 shows the relative intensity ratio of internal N (N_i) to surface N (N_f) dependent on etching time for the ZnO nanorods with NH_3 plasma treatment. No nitrogen signal was detected in the reference sample [see the inset of Fig. 3a] but the N1s peak could be detected in plasma-treated ZnO nanorods from surface to internal region for the ZnO nanorods (duration at 90 s). (Note: The N1s (~401 eV) internal signal was obtained by following the measurement steps. Firstly, ZnO nanorods were etched by Ar ion source and then the N1s signal of the etched ZnO nanorods can be detected. Next, both intensities of N1s signal (401 eV) for etched and non-etched nanorods were compared and considered as the internal and surface signals, respectively.) In addition, Fig. 3b illustrates the peak shift of 0.2–0.6 eV toward higher binding energies in Zn 2p spectrum for NH_3 plasma-treated ZnO nanorods as compared to that of the reference sample. This peak shift indicates the reduction of the surface band bending [13] and this may be related to the doping or incorporation of N ions into ZnO nanorods. The doped N atom could have the probability to occupy O sites to form the acceptor (N_O) in ZnO nanorods. Thus, the NH_3 plasma treatment seems to reduce the densities of the surface defects (Fig. 1b) on ZnO nanorods. However, it was also observed in the inset of Fig. 3b that as the ZnO nanorods were NH_3-plasma treated more than 180 s, the Zn 2p peak is shifted toward a higher binding energy around 4–5 eV.

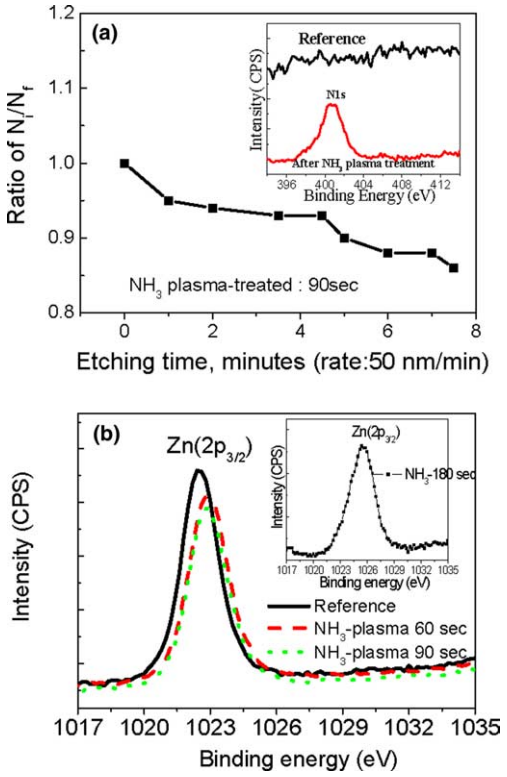

Fig. 3. (a) Dependence of relative intensity ratio of internal N (N_i) to surface N (N_f) on etching time for the ZnO nanorods with the inset showing the N1s spectra obtained from the ZnO nanorods with and without NH_3 plasma treatment (t = 90 s). (b) Zn 2p spectra obtained from the ZnO nanorods with and without NH_3 plasma treatment. The inset shows the Zn 2p3/2 spectra of ZnO nanorods with NH_3 plasma treatment of t = 180 s.

This phenomenon implies that the surface band bending of the ZnO nanorods was strongly influenced by NH_3 plasma treatment and therefore, the structure morphology of ZnO nanorods would be probably changed as shown in Fig. 2c.

Based on the above discussion, a mechanism for the formation of p-type ZnO nanorods under NH_3-plasma treatment is tentatively proposed as follows. As we can see in Fig. 1b, imperfect boundaries (surface roughness) and many defects (stacking faults) were observed in the ZnO nanorods where N and H radicals (ions) can be easily doped into ZnO nanorods by thermal diffusion via the nature defect routes. In general, the H ions are more easily diffused into ZnO than N ions in the plasma-treated process and can combine with other defects to form a shallow donor in ZnO. However, according to the PL analysis, it was found that the luminescence properties were enhanced with the increase of plasma-treated duration up to 90 s, indicating that the incorporation of H into ZnO nanorods does not show negative influence on the optical properties of ZnO nanorods in such short plasma duration. In other words, the improvement in optical property of ZnO nanorods can

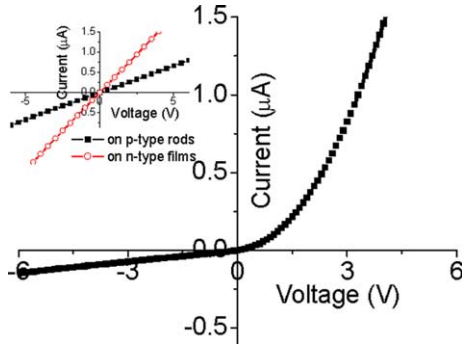

Fig. 4. I–V curves for a p–n homojunction formed by p-type ZnO nanorods grown on n-type ZnO films. Inset show the Ohmic contacts on n-type and p-type ZnO.

be primarily attributed to the reduction in surface defects and defect concentration of ZnO nanorods due to the occupation of N ions on the defect sites [14]. However, a long NH_3-Plasma treatment over 180 s not only causes the plasma etching but also promotes the diffusion of H ions into the ZnO nanorods as well as increases the concentration of shallow donors to restrict the formation of p-type ZnO.

Fig. 4 shows the I–V curve for a homojunction of p-type ZnO nanorods (treated by NH_3 plasma duration of 90 s) on n-type ZnO films. The graph in the inset of Fig. 4 shows surface I–V characteristics using In and Au/In electrodes on both n- and p-type ZnO. For the linear dependences of I–V characteristics, the ohmic contacts are fairly confirmed. Rectification by p–n junction is clearly displayed. The threshold voltage appears at 1.5 V under forward bias and it is almost half of the band gap energy of ZnO. It was also found that the I–V curve presents a little leakage current in reverse bias and this could be due to incomplete contact between some nanorods and contact metal electrode. Further experiments are required to understand the possible origin of the rectifying behavior with such a smaller threshold voltage. Nevertheless, the I–V characteristics of nitrogen-doped ZnO nanorods supports that the current approach is a valuable one to fabricate ZnO nanorods for p–n junction device application.

4. Conclusions

In summary, we have developed highly oriented p-type ZnO nanorods on a Si wafer buffered with ZnO film by combining NH_3 plasma treatment. The XPS analysis shows that the nitrogen ions can be doped into ZnO nanorods through surface adsorption or defect routes under NH_3 plasma treatment. The native defects of the ZnO nanorods can be effectively reduced and the optical property can be much improved. However, a longer plasma treatment would cause the morphology damage of ZnO nanorods and deteriorate their optical

property. The I–V results suggest that p-type ZnO nanorods with a smaller threshold voltage of 1.5 V can be obtained by combining the chemical solution process with NH_3 plasma treatment. These results demonstrate that this simple and low-cost process provides a promising option for large-scale production of the p–n junction ZnO optoelectronic devices.

Acknowledgement

The authors gratefully acknowledge the financial support of the National Science Council of Taiwan through Contract No. NSC-92-2216-E-009-014.

References

[1] Y. Cui, C.M. Liber, Science 291 (2001) 851.
[2] W.I. Park, G.-C. Yi, M. Kim, S.J. Pennycook, Adv. Mater. 15 (2003) 526.
[3] X. Duan, Y. Huang, Y. Cui, J. Wang, C.M. Lieber, Nature 409 (2001) 66.
[4] C.H. Liu, J.A. Zapien, Y. Yao, X.M. Meng, C.S. Lee, S.S. Fan, Y. Lifshitz, S.T. Lee, Adv. Mater. 15 (2003) 838.
[5] M.H. Huang, Y. Wu, H. Feick, N. Tran, E. Weber, P. Yang, Adv. Mater. 13 (2001) 113.
[6] W.T. Chiou, W.Y. Wu, J.M. Ting, Diam. Relat. Mater. 12 (10–11) (2003) 1841.
[7] L. Vayssieres, Adv. Mater. 15 (2003) 464.
[8] C.H. Liu, W.C. Yiu, F.C.K. Au, J.X. Ding, C.S. Lee, S.T. Lee, Appl. Phys. Lett. 83 (2003) 3168.
[9] Y.Q. Chang, D.B. Wang, X.H. Luo, X.Y. Xu, X.H. Chen, L. Li, C.P. Chen, R.M. Wang, J. Xu, D.P. Yu, Appl. Phys. Lett. 83 (2003) 4020.
[10] J.J. Wu, S.C. Liu, M.H. Yang, Appl. Phys. Lett. 85 (2004) 1027.
[11] S.C. Liou, C.S. Hsiao, S.Y. Chen, J. Cryst. Growth 274 (2004) 438.
[12] D.M. Bagnall, Y.F. Chen, Z. Zhu, T. Yao, Appl. Phys. Lett. 70 (1997) 2230.
[13] K. Ozawa, K. Edamoto, Surf. Sci. 524 (2003) 78.
[14] D. Li, Y.H. Leung, A.B. Djurisic, Z.T. Liu, M.H. Xie, S.L. Shi, S.J. Xu, W.K. Chen, Appl. Phys. Lett. 85 (2004) 1601.